Theoretical Prediction of the Photovoltaic Properties of BFBPD-$PC_{61}BM$ System as a Promising Organic Solar Cell

ZHAO Cai-Bin(赵蔡斌)[(1)];MA Jian-Qi(马剑琪)[(1)];GE Hong-Guang(葛红光)[(1)];TANG Zhi-Hua(唐志华)[(1)];JIN Ling-Xia(靳玲侠)[(1)];WANG Wen-Liang(王文亮)[(2)]

[(1)] *Shaanxi Key Laboratory of Catalysis, School of Chemical and Environmental Science, Shaanxi University of Technology, Hanzhong* 723001, *China*;[(2)] *Key Laboratory for Macromolecular Science of Shaanxi Province, School of Chemistry and Chemical Engineering, Shaanxi Normal University, Xi'an* 710062, *China*

ABSTRACT In this work, the photovoltaic properties of BFBPD-$PC_{61}BM$ system as a promising high-performance organic solar cell (OSC) were theoretically investigated by means of quantum chemistry and molecular dynamics calculations coupled with the incoherent charge-hopping model. Moreover, the hole carrier mobility of BFBPD thin-film was also estimated with the aid of an amorphous cell including 100 BFBPD molecules. Results revealed that the BFBPD-$PC_{61}BM$ system possesses a middle-sized open-circuit voltage of 0.70 V, large short-circuit current density of 17.26 mA cm^{-2}, high fill factor of 0.846, and power conversion efficiency of 10%. With the Marcus model, in the BFBPD-$PC_{61}BM$ interface, the exciton-dissociation rate, k_{dis}, was predicted to be 2.684×10^{13} s^{-1}, which is as 3～5 orders of magnitude large as the decay (radiative and non-radiative) one (10^{8}～10^{10} s^{-1}), indicating a high exciton-dissociation efficiency of 100% in the BFBPD-$PC_{61}BM$ interface. Furthermore, by the molecular dynamics simulation, the hole mobility of BFBPD thin-film was predicted to be as high as 1.265×10^{-2} $cm^2 \cdot V^{-1} s^{-1}$, which can be attributed to its dense packing in solid state.

Keywords: photovoltaic performances; theoretical prediction; carrier mobility; hopping mechanism;

DOI: 10.14102/j.cnki.0254-5861.2011-1659

1 INTRODUCTION

With the global fossil energy crisis intensified, the development of clean and renewable energy sources has gained widespread attention[1-3]. Relatively, as a clean, stable and renewable energy source, solar energy is an ideal alternative. In recent two decades, organic solar cell (OSC) has attracted intense interest owing to its specific advantages compared to the traditional photovoltaic technology, such as low-cost, solution process ability, light-weight, and the fabrication of flexible large-area devices[4-6]. Since the OSC was invented in 1991, tremendous efforts have been made to improve its performances. Nowadays, the power conversion efficiency (PCE) of OSC devices has been increased to 10%～12% or even higher[7], which brings out its broad

application prospect in the near future. In OSC devices the active layer is one of the most elements and plays very important roles, which is generally a blend composed by electron donor material and electron acceptor one. The electron donors mainly include organic small molecules and polymers with the strongly optical absorption, while the electron acceptor materials are usually fullerene derivatives, such as [6,6]-phenyl-C_{61}-butyric acid methyl ester ($PC_{61}BM$) and [6,6]-phenyl-C_{71}-butyric acid methyl ester ($PC_{71}BM$)[8, 9]. Although $PC_{61}BM$/$PC_{71}BM$ has several distinct disadvantages (such as low solubility in organic solvents, poor film forming nature, and weak light-harvesting) compared with those non-fullerene acceptors, the high electron affinity and electron mobility still make it a preferred electron donor in the development of high-performable OSC devices.

Recently, Cai et al. synthesized a novel small molecule material (BFBPD) with the donor-acceptor (D-A) character, and found that the BFBPD thin-film has high hole mobility as well as the prominent capture to solar radiation[10]. As a result, from the point of molecular properties, BFBPD is likely to be an excellent electron donor material. In this work, to seek novel OSC system, we carried out a computational investigation on the photovoltaic performances for the BFBPD-$PC_{61}BM$ system based on density functional theory (DFT) and time-dependent density functional theory (TD-DFT) calculations coupled with the incoherent charge-hopping transfer model. Main objectives of this work were to explore the possibility of BFBPD-$PC_{61}BM$ system as a potential high-performable OSC device by means of estimating those properties that are related to the PCE, such as open-circuit voltage, short-circuit current density, fill factor, exciton-dissociation/charge recombination rate, hole mobility, and so on. Results showed that as expected, the BFBPD-$PC_{61}BM$ system is a promising OSC candidate, and its PCE was predicted to be as high as 10%.

2 COMPUTATIONAL DETAILS

All the calculations were performed with density functional theory (DFT) and time-dependent density functional theory (TD-DFT) by means of the Gaussian 09 package[11]. The ground-state geometries were fully optimized without any symmetry constraints by the hybrid B3LYP functional[12] combined with 6-31G(d) basis set. Local minima were identified by frequency analysis at the same theoretical level. The absorption spectrum at the optimized ground-state geometry was calculated using the TD-MPW1PW91 method[13] and the 6-31G(d) basis set. To search for the most reasonable geometry of BFBPD-$PC_{61}BM$ complex, the detailed potential-surface scan was carried out between BFBPD and $PC_{61}BM$ with the CAM-B3LYP-D3(BJ)/ 6-311G(d,p) scheme[14, 15]. As seen in Fig. S1, the BFBPD-$PC_{61}BM$ complex was found to be most stable when the centroids distance of BFBPD and $PC_{61}BM$ is equal to 7.9 Å, which is in good agreement with the recent studies[16, 17]. Then, in subsequent calculations, the centroids distance of donor-acceptor complex was invariably fixed at 7.9 Å. In addition, we also considered the influence of molecular orientation on the geometry of donor-acceptor complex. As shown in Fig. S2, the molecular orientation affects a little on the studied complex. The inner reorganization energy in electron transfer process was estimated by the classical adiabatic potential energy surface method[18, 19], which has been verified to be accurate and has been used widely in numerous theoretical studies[20-24]. Meanwhile, the influence of solid stacking on the inner

reorganization energy was also considered by conductor-like polarizable continuum model (C-PCM)[25]. The effective electron coupling (V_{DA}) in Marcus model was calculated by means of the PW91PW91/6-31G(d) scheme[26, 27], which has been illustrated to provide the most accurate V_{DA} value at the DFT level[28, 29].

3 RESULTS AND DISCUSSION

The molecular structures and abbreviated notations for the studied compounds are depicted in Fig. 1.

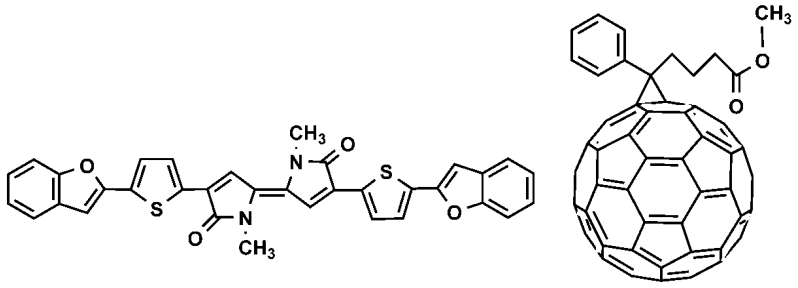

Fig. 1. Structures and abbreviated notations of studied compounds in this work

3. 1 Molecular geometries, electronic properties, and open circuit-voltage

As seen in Fig. S3, our optimization revealed that BFBPD molecule keeps a good planar geometry, and the dihedral angle between diketopyrrolopyrrole (DPP) and thiophene units is about 19.5°, and it remarkably withdraws to 1.5° between benzofuran and thiophene, which indicates that BFBPD has good electronic delocalization. Fig. 2 shows the HOMO and LUMO for BFBPD, $PC_{61}BM$, and BFBPD-$PC_{61}BM$ complexes. As seen, in BFBPD molecule both the HOMO and LUMO mainly distribute on the molecular core and the contribution from the benzofuran is small, indicating the frontier molecular orbital is mainly determined by the core, instead of the benzofuran unit. In addition, it can be noticed that the CH_3 located in DPP unit contributes nothing to both HOMO and LUMO, denoting the CH_3 has no influence on the frontier molecular orbital and electronic properties of BFBPD, verifying it is very rational to replace 2-ethylhexyl with the CH_3 in this work. Similarly, the methyl-4-phenylbutanoate contributes also small to both HOMO and LUMO in $PC_{61}BM$, meaning the substituent only enhances the C_{60} solubility, and has no influence on its electronic properties, which is in good agreement with the previous experimental studies[30, 31]. As for BFBPD-$PC_{61}BM$ complex, the HOMO and LUMO exhibit an obvious separation characteristic, and the HOMO completely locates on the BFBPD, while the LUMO mainly centuries on the $PC_{61}BM$, which suggests the easy formation of BFBPD$^{\bullet+}$-$PC_{61}BM^{\bullet-}$ charge-separated state.

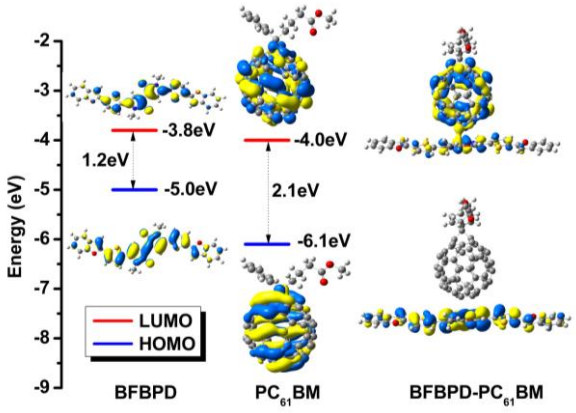

Fig. 2. HOMO and LUMO of BFBPD, $PC_{61}BM$, and BFBPD-$PC_{61}BM$ complex

According to the previous study, the open circuit-voltage (V_{oc}) for OSCs can be estimated with[32],

$$V_{oc} = (1/e)(|E_{HOMO}(\mathrm{D})| - |E_{LUMO}(\mathrm{A})|) - 0.3 \qquad (1)$$

where $E_{HOMO}(D)/E_{LUMO}(A)$ is the HOMO/LUMO level of donor/acceptor, e is the electron charge, and the value of 0.3 is an empirical factor. Then, based on the experiment HOMO (–5.0 eV[10]) for BFBPD and LUMO (–4.0 eV [33, 34]) for $PC_{61}BM$, the V_{oc} was estimated to be 0.70 V for the BFBPD-$PC_{61}BM$ system. Moreover, we also estimated the PCE for the BFBPD-$PC_{61}BM$ system by means of the Scharber diagram. As shown in Fig. 3, the PCE of BFBPD-$PC_{61}BM$ system was predicted to be 10%, which indicates its excellent photovoltaic performances.

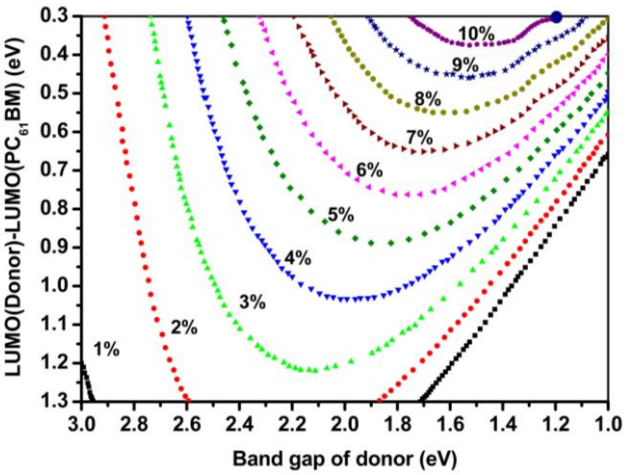

Fig. 3. Predicted PCE for BFBPD-$PC_{61}BM$ cell with the Scharber diagram

3. 2 Exciton binding energy and optical absorption properties

As is well-known, the exciton binding energy (E_b) is one of the most parameters, which is directly related to the exciton-separation efficiency. Usually, the E_b is taken as the difference between the transport gap (E_t) and the optical band gap (E_{opt}). The former is the difference between the adiabatic ionization potential (E_{AIP}) and electron affinity (E_{AEA}) of donor in solid state, while the latter is the first-singlet emission energy (E_m). Then, the E_b can be calculated as the following expression[35],

$$E_b = E_{AIP} - E_{AEA} - E_m \quad (2)$$

where E_{AIP} and E_{AEA} are the adiabatic ionization potential (AIP) and adiabatic electron affinity (AEA) of donor material, and E_m is the lowest-singlet emission energy. As seen in Eq. (2), to calculate the E_b, the E_{AIP} and E_{AEA} of donor in solid state firstly need to be calculated. In this work, the E_{AIP}/E_{AEA} of solid BFBPD was estimated via the method reported by Schwenn et al.[36], which has been verified to be a good scheme that estimates the electronic properties of organic materials in solid state.

Table 1. Calculated E_{AIP}, E_{AEA}, and E_b Values in Gas/Solid State for BFBPD with Two Different DFT Methods (eV)

Method	B3LYP/6-311G(d,p)				CAM-B3LYP/6-311G(d,p)			
	E_{AIP}	E_{AEA}	E_m	E_b	E_{AIP}	E_{AEA}	E_m	E_b
Gas state	5.745	2.248	1.358	2.139	6.012	2.141	1.664	2.207
Solid state	5.001	3.232	1.343	0.427	5.230	3.201	1.348	0.681
P^+/P^- [a]	0.744	0.984	/	/	0.782	1.060	/	/

[a] The P^+/P^- represents the cation/anion polarization energy.

Table 1 lists the E_{AIP}/E_{AEA} values for BFBPD in gas/solid state calculated with two different DFT methods. It can be noted that the E_b was estimated to be 2.139/2.207 eV in gas phase, which is unusually larger than the measured values of 0.2～1.0 eV in numerous organic materials[37], indicating the solid stacking maybe has quite strong influence on the electronic properties of organic materials. Calculated cation/anion polarization energy (P_+/P_-) verifies our speculation. As seen, the P_+/P_- is as high as 0.744/0.984 eV, indicating it is essential to consider the solid stacking effect for accurately estimating the E_b in theoretical study. Compared the E_{AIP}/E_{AEA} values in gas phase to those in solid state, it can be noticed that in gas phase the E_{AIP} is larger, while the E_{AEA} is smaller, which is similar to the measured and theoretical results in acenes[38]. According to calculated E_{AIP}, E_{AEA}, and E_m for the solid BFBPD, the E_b was estimated to be about 0.427 eV. The precious study showed that the exciton is unstable if $E_b < k_BT$, which amounts to 0.025 eV at room temperature[39]. According to the calculated E_b for the BFBPD solid, it can be deduced that the photo-induced exciton in BFBPD is relatively stable, which can be efficiently transported to the BFBPD-$PC_{61}BM$ interface without rapidly being decayed in transit.

As we know, the strong harvest to solar radiation is very important for high-performable donor materials, which directly determines the short-circuit current density. To explore reliable TD-DFT methods estimating optical absorption properties for BFBPD, a set of popular DFT methods were tested. As seen in Table S1, compared with the experimental value, the TD-MPW1PW91/6-31G(d)[40] scheme can accurately estimate the excited energy of BFBPD, and the derivation between the theoretical and experimental values is only about 1.0 nm (about 2.0×10^{-4} eV). Moreover, the full absorption spectrum of BFBPD was also simulated. As seen in Fig. S4, in UV-vis region the simulated spectrum for BFBPD is in excellent agreement with the experimental one, indicating the TD-MPW1PW91/6-31G(d) scheme is reliable to estimate the light absorption and subsequent short-circuit current density. In addition, it can be noticed in Table S2 that the strongest absorption for BFBPD molecule can be assigned to the π-π* type, and dominated completely by the electron transition of

HOMO → LUMO (~100%).

3. 3 Short-circuit current density J_{sc}, Fill factor *FF*, and PCE η

The short-circuit current density, J_{sc}, is another key parameter that determines the PCE of OSC devices, which can be expressed as[41, 42],

$$J_{sc} = q\int_0^{\infty} \eta_{IQE}(\lambda) \times S(\lambda) d\lambda \tag{3}$$

where $S(\lambda)$ is the incident photon-to-current conversion efficiency at a fixed wavelength, q is the unit charge, and $\eta_{IEQ}(\lambda)$ is the internal quantum efficiency. The $\eta_{IEQ}(\lambda)$ term can be described as the product of η_{λ} (light-harvesting efficiency), η_{CT} (charge transfer efficiency), and η_{coll} (charge collection efficiency),

$$\eta_{IQE} = \eta_{\lambda}\eta_{CT}\eta_{coll} \tag{4}$$

The η_{λ} can be calculated by $\eta_{\lambda} = 1 - 10^{-f}$, where f is the oscillator strength. Then, to estimate the maximum J_{sc}, we sent the $\eta_{CT} = 1.0$ and $\eta_{coll} = 1.0$. Our calculation showed that the f is about 1.4692 at the lowest-excited singlet state for BFBPD, then yielding $\eta_{\lambda} = 0.770$. Fig. 4 shows the simulated $\eta_{IEQ}(\lambda)$ and J_{sc} with the above-mentioned parameters. As seen, the J_{sc} for the BFBPD-$PC_{61}BM$ system was predicted to be as high as 17.26 mA·cm^{-2}, which can be attributed to the BFBPD strong spectral response. In addition, it can be noticed that the $\eta_{IEQ}(\lambda)$ is as large as 81.7% in the visible region. Relatively, BFBPD exhibits a weak capture for the ultraviolet radiation ($\eta_{IEQ}(\lambda) \approx 57\%$). For the *FF* calculation, an approximate scheme can be expressed as[43, 44],

$$FF = \frac{v_{oc} - \ln(v_{oc} + 0.72)}{v_{oc} + 1} \tag{5}$$

where v_{oc} is the dimensionless voltage, which can be estimated with the V_{oc}[45, 46],

$$v_{oc} = \frac{qV_{oc}}{nk_BT} \tag{6}$$

where k_B, T and q are Boltzmann constant, temperature (here, we set T = 300 K), and elementary charge respectively, n is an ideality factor relating to an ideal (n = 1) or non-ideal (n > 1) diode[47], organic solar cells typically have ideality factors in the range of 1.5～2.0 due to their inherent disorder in solid state[48]. According to the calculated V_{oc} (0.70 V) for the BFBPD-$PC_{61}BM$ system, the v_{oc} was estimated to be 27.08 at n = 1.0 and 13.54 at n = 2, then, the *FF* for BFBPD-$PC_{61}BM$ was predicted to be as high as 0.748 (n = 2.0) and 0.846 (n = 1.0), in excellent agreement with measured values in most OSC devices. According to the previous study, the PCE (η) of OSC devices can be estimated with the following equation[49, 50],

$$\eta = \frac{P_{\max}}{P_{in}} = \frac{V_{oc}J_{sc}}{P_{in}}FF \tag{7}$$

where $P_{\max}$ and P_{in} (= 100 mW·cm^{-2}) are the maximum and incident power, respectively. With the calculated V_{oc}, J_{sc}, and *FF*, the PCE of BFBPD-$PC_{61}BM$ system was predicted to be 9.23% (n = 2.0) and 10.22% (n = 1.0), which is in excellent agreement with the estimated value (~10%) by means of the Scharber diagram.

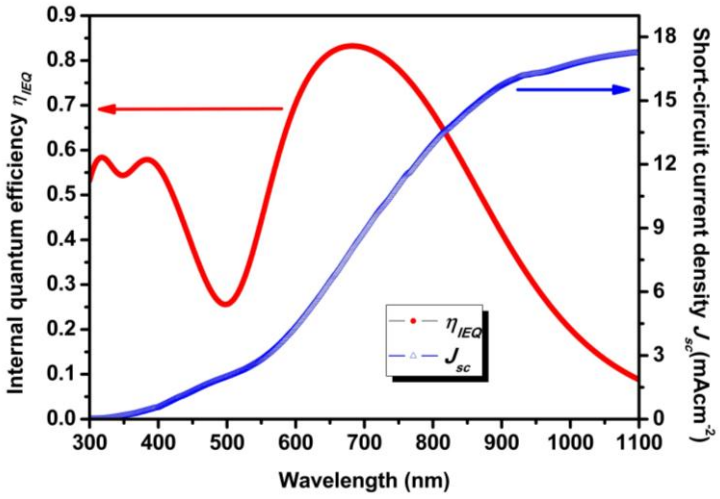

Fig. 4. Simulated $\eta_{IEQ}(\lambda)$ and J_{sc} for the BFBPD-PC$_{61}$BM system

3. 4 Gibbs free energies and reorganization energies in exciton-dissociation and charge-recombination

The change of Gibbs free energy (ΔG) in charge transfer process can be estimated as the energy difference in the final and initial states, accounting for the Coulombic attraction between two opposite charges in charge-separated state. Thus, for the exciton-dissociation, the ΔG (ΔG_{dis}) can be written as[51],

$$\Delta G_{dis} = E_D^+(Q^+) + E_A^-(Q^-) - E_D^*(Q^*) - E_A^0(Q^0) + \Delta E_{coul} \quad (8)$$

where $E_D^*(Q^*)/E_D^+(Q^+)$ is the total energy of isolated donor in its equilibrium geometry of the lowest singlet-excited/cationic state, $E_A^-(Q^-)/E_A^0(Q^0)$ is the total energy of isolated acceptor in its equilibrium geometry of anionic/neutral state, and ΔE_{coul} is the Coulombic attraction between donor and acceptor in charge-separated state, which can be estimated with the flowing equation,

$$\Delta E_{coul} = \sum_{D^+}\sum_{A^-}\frac{q_{D^+}q_{A^-}}{4\pi\varepsilon_0\varepsilon_s r_{D^+A^-}} - \sum_{D^*}\sum_{A}\frac{q_{D^*}q_A}{4\pi\varepsilon_0\varepsilon_s r_{D^*A}} \quad (9)$$

where q_D and q_A are the atomic charge on donor and acceptor in their relevant states with a separation distance, r_{DA}. The ε_0 is the vacuum dielectric constant (8.854×10^{-12} F m^{-1}), and ε_s is the static dielectric constant of medium. Similarly, the Gibbs free energy change (ΔG_{rec}) in charge recombination can also be estimated with the expression similar to Eqs. (8) and (9). Here, the ε_s was estimated with the Clausius-Mossotti equation[52],

$$\varepsilon_s = \left(1+\frac{8\pi\bar{\alpha}}{3V}\right)\left(1-\frac{4\pi\bar{\alpha}}{3V}\right)^{-1} \quad (10)$$

where V is the Connolly molecular volume, $\bar{\alpha}$ is the isotropic component of molecular polarizability, $\bar{\alpha} = \frac{1}{3}\sum_i \alpha_{ii}$, and α_{ii} is the diagonal matrix elements of the first-order polarizability tensor. Calculations showed that ε_s is 3.653 for BFBPD, which is in good accordance with the measured values (ranging from 2.0 to 5.0[53, 54]) in most organic materials. As for PC$_{61}$BM, the experimental ε_s value of 3.9[55] was used in this work. The total ε_s of BFBPD-PC$_{61}$BM system was taken as an average of their respective contribution. Our calculation showed that the ΔG_{dis} is about –0.476 eV, while the ΔG_{rec} decreases to –0.720 eV. Obviously, the ΔG_{dis} and ΔG_{rec} were calculated to be negative, denoting that the exciton-dissociation and charge-recombination are favorable in

thermodynamics. In addition, the smaller ΔG_{rec} indicates a larger driving force in charge-recombination process.

Generally, in organic solids the total reorganization energy (λ) of electron transfer can be divided into two sections, namely the internal reorganization energy (λ_{int}) and the external one (λ_{ext}). In the case of charge dissociation, the λ_{int} is taken as an average of the following λ_1 and λ_2[56],

$$\lambda_1 = [E_D^*(Q^+) + E_A^0(Q^-)] - [E_D^*(Q^*) + E_A^0(Q^0)] \quad (11)$$

$$\lambda_2 = [E_D^+(Q^*) + E_A^-(Q^0)] - [E_D^+(Q^+) + E_A^-(Q^-)] \quad (12)$$

where $E_D^*(Q^*)/E_D^*(Q^+)$ is the energy of donor in the lowest excited-state with the equilibrium geometry of excited/cationic state, $E_D^+(Q^*)/E_D^+(Q^+)$ is the energy of donor in the cationic state with the equilibrium geometry of excited/cationic state, $E_A^0(Q^-)/E_A^0(Q^0)$ is the energy of acceptor in the neutral state with the equilibrium geometry of anion/neutral state, and $E_A^-(Q^0)/E_A^-(Q^-)$ is the energy of acceptor in the anionic state with the equilibrium geometry of neutral/anionic state. Our calculation showed that the λ_{int} (λ_{dis}) is 0.119 eV in charge-dissociation process for BFBPD-$PC_{61}BM$, which remarkably increases to 0.189 eV in the case of charge recombination. Compared to the λ_{int}, the λ_{ext} is difficult to accurately calculate. Here, we used the classical dielectric continuum model initially developed by Marcus for the electron-transfer reaction between spherical ions in solution to estimate λ_{ext}. According to this model, the λ_{ext} term is given by[57],

$$\lambda_{ext} = \frac{(\Delta e)^2}{8\pi\varepsilon_0}\left(\frac{1}{\varepsilon_{op}} - \frac{1}{\varepsilon_s}\right)\left(\frac{1}{R_D} + \frac{1}{R_A} - 2\sum_D\sum_A \frac{q_D q_A}{r_{DA}}\right) \quad (13)$$

where ε_{op} is the optical dielectric constant of medium, R_D (= 6.30 Å for BFBPD) and R_A (= 6.50 Å for $PC_{61}BM$) are the effective radii of donor and acceptor estimated as the radius of sphere having the same surface as the surface accessible area of molecule. The q_D and q_A denote the atomic charges on the ions. The ε_{op} can be estimated with the Lorentz-Lorenz equation[58, 59],

$$\varepsilon_{op} = n^2 = \frac{V_m + 2R}{V_m - R} \quad (14)$$

where n is the refractive index, V_m is the molar volume (V_m = M/ρ, where M is the molar mass, and ρ is the density of material.), and R is the molar refraction. Here, the ρ was estimated with the molecular dynamics method, and the simulated detail is shown in the supporting information. Our results showed the ε_{op} and ρ for BFBPD are 1.523 and 1.334 g cm^{-3}, respectively. As for $PC_{61}BM$, the experimental refractive index (n = 1.866) was used to estimate ε_{op}, which is equal to 3.482 according to our calculation. With the above-mentioned parameters, the λ_{ext} was estimated to be equal to 0.239 eV. In summary, λ = 0.512 eV in charge-dissociation process for BFBPD-$PC_{61}BM$ system, which remarkably increases to 0.582 eV for the charge-recombination process.

3. 5 Electron couplings and exciton-dissociation/charge-recombination recombination rate

The V_{DA} is an important parameter that determines the charge transfer rate constant (k_{DA}). In this work, the direct-coupling (DC) method was used to estimate the V_{DA}[60, 61]. In terms of this scheme, the V_{DA} can be calculated by the following expression[62, 63],

$$V_{D(i)A(j)} = \frac{T_{D(i)A(j)} - 0.5(e_{D(i)} + e_{A(j)})S_{D(i)A(j)}}{1 - S^2_{D(i)A(j)}} \quad (15)$$

where $T_{D(i)A(j)}$ is the electron coupling of the *i*th molecular orbital of donor and the *j*th molecular orbital of acceptor, $S_{D(i)A(j)}$ is the spatial overlap integral, and $e_{D(i)}/e_{A(j)}$ is the site energy. The $T_{D(i)A(j)}$, $S_{D(i)A(j)}$, and $e_{D(i)}/e_{A(j)}$ can be obtained from the $T_{D(i)A(j)} = \langle\psi_{D(i)}|F^{KS}|\psi_{A(j)}\rangle$, $S_{D(i)A(j)} = \langle\psi_{D(i)}|\psi_{A(j)}\rangle$, and $e_{D(i)}/e_{A(j)} = \langle\psi_{D(i)}/\psi_{A(j)}|F^{KS}|\psi_{D(i)}/\psi_{A(j)}\rangle$. Among them, $\psi_{D(i)}$ is the HOMO (for charge-recombination) or LUMO (for charge-dissociation) of donor, $\psi_{A(j)}$ is the LUMO of acceptor, and F^{KS} is the Kohn-Sham matrix of donor-acceptor system.

$$F^{KS} = SC\varepsilon C^{-1} \quad (16)$$

where S is the intermolecular overlap matrix, C is the molecular orbital coefficient matrix from the isolated monomer, and ε is the orbital energy from one-step diagonalization without iteration. Generally, the V_{DA} in the exciton-dissociation process is taken as the coupling between the LUMO of donor and acceptor. However, since the LUMO+1 and LUMO+2 in $PC_{61}BM$ are degenerated energetically with its LUMO[64], the V_{DA} between the LUMO of BFBPD and LUMO+1/LUMO+2 of $PC_{61}BM$ was also computed. Finally, the average V_{DA} was used to calculate the k_{DA}. As for the charge-recombination, the same treatment was done. Our results showed that the V_{DA} is about 0.034 eV in exciton dissociation, which decreases to 0.026 eV in charge recombination. At high temperature and weak coupling limits, the charge transfer in organic materials involves a thermally activated hopping mechanism. According to the Marcus theory[65, 66], the k_{DA} can be expressed as

$$k_{DA} = \frac{V_{DA}^2}{\mathrm{h}}\left(\frac{\pi}{\lambda k_B T}\right)^{1/2} \exp\left[-\frac{(\Delta G + \lambda)^2}{4\lambda k_B T}\right] \quad (17)$$

where λ is the total reorganization energy, V_{DA} is the effective electron coupling, T is the temperature, $\hbar$ and k_B are the reduced Planck and Boltzmann constants respectively, and ΔG is the change of Gibbs free energy between the final state and first one. Based on the calculated λ and V_{DA}, the exciton-dissociation (k_{dis}) and charge-recombination (k_{rec}) rate constants were estimated to be as high as 2.684×10^{13} and 1.108×10^{13} s^{-1} respectively in BFBPD-$PC_{61}BM$ interface. Recent studies have illustrated that the decay rate constant (k_d) of excited organic molecules typically ranges 1.0×10^8 to 1.0×10^{10} s^{-1}[67]. Our results showed that the k_{dis} is larger 3～5 orders of magnitude than the k_d, which indicates very high exciton-dissociation efficiency (~100%) in the BFBPD-$PC_{61}BM$ interface. In addition, although the k_{rec} is relatively larger, the charge-recombination efficiency is still very low. According to previous studies, the electron transferred onto $PC_{61}BM$ can be rapidly converted to the triplet state from the singlet state[68, 69], which remarkably hinders from the recombination of free carriers.

3. 6 Hole transfer rate and hole mobility in BFBPD thin-film

As is known to all, the charge transport ability of donor remarkably affects the solar cell's performance. Thus, it is essential to estimate charge transport properties of BFBPD thin-film. The charge transport ability in organic materials can be chartered with its carrier mobility (μ), which can be calculated by means of the Einstein-Smoluchowski equation[70, 71],

$$\mu = \frac{eD}{k_B T} \quad (18)$$

where D is diffusion coefficient, e is elementary charge, k_B is Boltzmann constant, and T is temperature, respectively. The D can be estimated by means of the following appropriate relation[72, 73],

$$D \approx \frac{1}{2n}\sum_i d_i^2 k_i P_i \tag{19}$$

where n is the spatial dimensionality, which is 3 for organic solids, d_i is the centroids distance of the ith hopping dimer, k_i is the charge transfer rate constant, and P_i ($P_i = k_i/\Sigma_i k_i$) is the hopping probability. In this work, the charge mobility of BFBPD thin-film was evaluated by means of an amorphous cell with 100 BFBPD molecules built by means of the molecular dynamics simulation. As seen in Fig. 5, our result showed that the BFBPD molecules in solid state exhibit a close-packed pattern, which is favorable for the hole-carrier transfer.

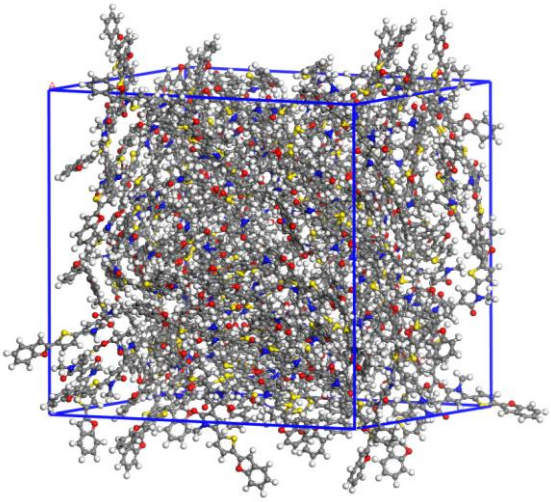

Fig. 5. Optimized amorphous cell with 100 BFBPD molecules

Table 2 shows the calculated λ_{int} term for BFBPD in hole transfer with two different DFT methods. As seen, the CAM-B3LYP/6-31G(d) scheme presented quite large λ_{int} values due to considering the long-range correlation effect. In addition, it can be noticed that the λ_{int} in solid state is obviously smaller than that in gas phase, denoting that the solid stack, to some extent, limits the structural relaxation of BFBPD molecule in charge transfer process. Since the donor materials in OSC devices usually keep in solid state under operating conditions, the λ_{int} estimated by means of the solid state model is more reasonable and reliable.

Table 2. Calculated λ_{int} for BFBPD with Two Different DFT Methods (eV)

Method	B3LYP/6-311G(d,p)			CAM-B3LYP/6-311G(d,p)		
	λ_1[a]	λ_2[b]	λ_{int}	λ_1[a]	λ_2[b]	λ_{int}
Gas state	0.176	0.217	0.393	0.409	0.355	0.764
Solid state	0.168	0.209	0.377	0.385	0.337	0.722

[a] λ_1 is the structural relaxation energy from neutral state to cation state. [b] λ_2 is the structural relaxation energy from cation state to neutral state.

To explore possible charge transfer dimers, 20 molecular pairs with relatively larger V_{DA} values were abstracted from the optimized amorphous cell, and their geometries, centroids distances, as well as estimated V_{DA} values are shown in Table S3. Based on λ_{int} in the solid state and V_{DA} values, the hole carrier mobility (μ_h)

of solid BFBPD thin-film was estimated to be as high as 1.265 × 10^{-2} $cm^2 \cdot V^{-1} s^{-1}$, which is in excellent agreement with its measured value of $3.7\times10^{-3} \sim 9.0\times10^{-2}$ $cm^2 \cdot V^{-1} s^{-1}$[10]. According to the previous investigation, for high-performance electron donor materials, the μ_h should be not less than 10^{-3} $cm^2 \cdot V^{-1} \cdot s^{-1}$[32]. Our result showed as a potential donor material, the BFBPD can satisfy the requirement that rapidly transports holes.

4 CONCLUSION

In this work, with DFT/TD-DFT calculations, the photovoltaic properties of BFBPD-$PC_{61}BM$ system were theoretically investigated. Results revealed that the BFBPD-$PC_{61}BM$ system possesses middle-sized open-circuit voltage of 0.70 V, large short-circuit current density of 17.26 mA cm^{-2}, high fill factor of 0.846 and power conversion efficiency of 10%. Based on the Marcus charge transfer model, the k_{dis}(2.684 × 10^{13} s^{-1}) was estimated to be larger 3～5 orders of magnitude than the k_d(1.0 × 10^8 to 1.0 × 10^{10} s^{-1}), which indicates very high exciton-dissociation efficiency (~100%) in the BFBPD-$PC_{61}BM$ interface. Moreover, with an amorphous cell optimized by molecular dynamics method, the hole carrier mobility for BFBPD thin-film was predicted to be as high as 1.265 × 10^{-2} $cm^2 \cdot V^{-1} s^{-1}$ at room temperature. In brief, our calculations showed that BFBPD is an excellent electron donor material, and the BFBPD-$PC_{61}BM$ system is a promising OSC candidate. However, these results need to be confirmed by experiments.

REFERENCES

(1) Slota, J. E.; He, X.; Huck, W. T. S. Controlling nanoscale morphology in polymer photovoltaic devices. *Nanotoday*. **2010**, 5, 231–242.

(2) Chi, Y.; Chou, P. T. Transition-metal phosphors with cyclometalating ligands: fundamentals and applications. *Chem. Soc. Rev*. **2010**, 39, 638–655.

(3) Vilaca, G.; Jousseaume, B.; Mahieux, C.; Belin, C.; Cachet, H.; Beranrd, M. C.; Vivier, V.; Toupance, T. Tin dioxide materials chemically modified with trialkynylorganotins: functional nanohybrids for photovoltaic applications. *Adv. Mater.* **2006**, 18, 1073–1077.

(4) Coakley, K. M.; McGehee, M. D. Conjugated polymer photovoltaic cells. *Chem. Mater.* **2004**, 16, 4533–4542.

(5) Thompson, B. C.; Frechet, J. M. J. Polymer-fullerene composite solar cells. *Angew. Chem. Int. Ed.* **2008**, 47, 58–77.

(6) Kippelen, B.; Brédas, J. L. Organic photovoltaics. *Energy Environ. Sci.* **2009**, 2, 251–261.

(7) Li, N.; Baran, D.; Forberich, K.; Machui, Ameri, F. T.; Turbiez, M.; Carrasco-Orozco, M.; Drees, M.; Facchetti, A.; Krebse, F. C.; Brabeca, C. J. Towards 15% energy conversion efficiency: a systematic study of the solution-processed organic tandem solar cells based on commercially available materials. *Energy Environ. Sci.* **2013**, 6, 3407–3413.

(8) Brabec, C. J.; Gowrisanker, S.; Halls, J. J. M.; Laird, D.; Jia, S.; Williams, S. P. Polymer-fullerene bulk-heterojunction solar cells. *Adv. Mater.* **2010**, 22, 3839–3856.

(9) Lenes, M.; Wetzelaer, G. J. A. H.; Kooistra, F. B.; Veenstra, S. C.; Hummelen, J. C.; Blom, P. W. M. Fullerene bisadducts for enhanced open-circuit voltages and efficiencies in polymer solar cells. *Adv. Mater.* **2008**, 20, 2116–2119.

(10) Cai, Z.; Guo, Y.; Yang, S.; Peng, Q.; Luo, H.; Liu, Z.; Zhang, G.; Liu, Y.; Zhang, D. New donor-acceptor-donor molecules with pechmann dye as the core moiety for solution-processed good-performance organic field-effect transistors. *Chem. Mater.* **2013**, 25, 471–478.

(11) Frisch, M. J.; Trucks, G. W.; Schlegel, H. B.; Scuseria, G. E.; Robb, M. A.; Cheeseman, J. R.; Scalmani, G.; Barone, V.; Mennucci, B.; Petersson, G. A.; Nakatsuji, H.; Caricato, M.; Li, X.; Hratchian, H. P.; Izmaylov, A. F.; Bloino, J.; Zheng, G.; Sonnenberg, J. L.; Hada, M.; Ehara, M.; Toyota, K.; Fukuda, R.; Hasegawa, J.; Ishida, M.; Nakajima, T.; Honda, Y.; Kitao, O.; Nakai, H.; Vreven, T.; Montgomery, J. A., Jr.; Peralta, J. E.; Ogliaro, F.; Bearpark, M.; Heyd, J. J.; Brothers, E.; Kudin, K. N.; Staroverov, V. N.; Kobayashi, R.; Normand, J.; Raghavachari, K.; Rendell, A.; Burant, J. C.; Iyengar, S. S.; Tomasi, J.; Cossi, M.; Rega, N.; Millam, J. M.; Klene, M.; Knox, J. E.; Cross, J. B.; Bakken, V.; Adamo, C.; Jaramillo, J.; Gomperts, R.; Stratmann, R. E.; Yazyev, O.; Austin, A. J.; Cammi, R.; Pomelli, C.; Ochterski, J. W.; Martin, R. L.; Morokuma, K.; Zakrzewski, V. G.; Voth, G. A.; Salvador, P.; Dannenberg, J. J.; Dapprich, S.; Daniels, A. D.; Farkas, Ö.; Foresman, J. B.; Ortiz, J. V.; Cioslowski, J.; Fox, D. J. Gaussian, Inc., Pittsburgh PA **2009**, *Gaussian 09, Revision C.01*.

(12) Becke, A. D. Density-functional thermochemistry. III. The role of exact exchange. *J. Chem. Phys.* **1993**, 98, 5648–5652.

(13) Adamo, C.; Barone, V. Exchange functionals with improved long-range behavior and adiabatic connection methods without adjustable parameters: The mPW and mPW1PW models. *J. Chem. Phys.* **1998**, 108, 664–675.

(14) Yanai, T.; Tew, D. P.; Handy, N. C. A new hybrid exchange-correlation functional using the Coulomb-attenuating method (CAM-B3LYP). *Chem. Phys. Lett.* **2004**, 393, 51–57.

(15) Aidas, K.; Møgelhøj, A.; Nilsson, E. J. K.; Johnson, M. S.; Mikkelsen, K. V.; Christiansen, O.; Söderhjelm, P.; Kongsted, J. On the performance of quantum chemical methods to predict solvatochromic effects: the case of acrolein in aqueous solution. *J. Chem. Phys.* **2008**, 128, 194503–15.

(16) Liu, T.; Troisi, A. Absolute rate of charge separation and recombination in a molecular model of the P3HT/PCBM interface. *J. Phys. Chem. C* **2011**,115, 2406–2415.

(17) Zhao, C.; Wang, Z.; Zhou, K.; Ge, H.; Zhang, Q.; Jin, L.; Wang, W.; Yin, S. Theoretical investigation on photovoltaic properties of BDT and DPP copolymer as a promising organic solar cell. *Acta Chim. Sinica* **2016**, 74, 251–258.

(18) Malagoli, M.; Brédas, J. L. Density functional theory study of the geometric structure and energetics of triphenylamine-based hole-transporting molecules. *Chem. Phys. Lett.* **2000**, 327, 13–17.

(19) Lemaur, V.; da Silva Filho, D. A.; Coropceanu, V.; Lehmann, M.; Geerts, Y.; Piris, J.; Debije, M. G.; van de Craats, A. M.; Senthilkumar, K.; Siebbeles, L. D. A.; Warman, J. M.; Brédas, J. L.; Cornil, J. Charge transport properties in discotic liquid crystals: a quantum-chemical insight into structure-property relationships. *J. Am. Chem. Soc.* **2004**, 126, 3271–3279.

(20) Wang, L.; Nan, G.; Yang, X.; Peng, Q.; Li, Q.; Shuai, Z. Computational methods for design of organic materials with high charge mobility. *Chem. Soc. Rev.* **2010**, 39, 423–434.

(21) Yong, X.; Zhang, J. A rational design strategy for donors in organic solar cells: the conjugated planar molecules possessing anisotropic multibranches and intramolecular charge transfer. *J. Mater. Chem.* **2011**, 21, 11159–11166.

(22) Jin, R.; Ahmad, I. Theoretical study on photophysical properties of multifunctional star-shaped molecules with 1,8-naphthalimide core for organic light-emitting diode and organic solar cell application. *Theor. Chem. Acc.* **2015**, 134, 89.

(23) Coropceanu, V.; Cornil, J.; da Silva Filho, D. A.; Olivier, Y.; Silbey, R.; Brédas, J. L. Charge transport in organic semiconductors. *Chem. Rev.* **2007**, 107, 926–952.

(24) Yang, X.; Wang, L.; Wang, C.; Long, W.; Shuai, Z. Influences of crystal structures and molecular sizes on the charge mobility of organic semiconductors: oligothiophenes. *Chem. Mater.* **2008**, 20, 3205–3211.

(25) Tomasi, J.; Mennucci, B.; Cammi, R. Quantum mechanical continuum solvation models. *Chem. Rev.* **2005**, 105, 2999–3094.

(26) Mohakud, S.; Alex, A. P.; Pati, S. K. Ambipolar charge transport in α-oligofurans: a theoretical study. *J. Phys. Chem. C* **2010**, 114, 20436–20442.

(27) Troisi, A.; Orlandi, G. Dynamics of the intermolecular transfer integral in crystalline organic semiconductors. *J. Phys. Chem. A* **2006**, 110, 4065–4070.

(28) Song, Y.; Di, C.; Yang, X.; Li, S.; Xu, W.; Liu, Y.; Yang, L.; Shuai, Z.; Zhang, D.; Zhu, D. A cyclic triphenylamine dimer for organic field-effect transistors with high performance. *J. Am. Chem. Soc.* **2006**, 128, 15940–15941.

(29) Huang, J.; Kertesz, M. Intermolecular transfer integrals for organic molecular materials: Can basis set convergence be achieved? *Chem. Phys. Lett.* **2004**, 390, 110–115.

(30) Zheng, L.; Zhou, Q.; Deng, X.; Yuan, M.; Yu, G.; Cao, Y. Methanofullerenes used as electron acceptors in polymer photovoltaic devices. *J. Phys. Chem. B* **2004**, 108, 11921–11926.

(31) Wang, X.; Guo, Y.; Xiao, Y.; Zhang, L.; Yu, G.; Liu, Y. Synthesis and characterization of fullerene derivatives with perfluoroalkyl groups. *J. Mater. Chem.* **2009**, 19, 3258–3262.

(32) Scharber, M. C.; Mühlbacher, D.; Koppe, M.; Denk, P.; Waldauf, C.; Heeger, A. J.; Brabec, C. J. Design rules for donors in bulk-heterojunction solar cells-towards 10% energy-conversion efficiency. *Adv. Mater.* **2006**, 18, 789–794.

(33) Hummelen, J. C.; Knight, B. W.; LePeq, F.; Wudl, F.; Yao, J.; Wilkins, C. L. Preparation and characterization of fulleroid and methanofullerene derivatives. *J. Org. Chem.* **1995**, 60, 532–538.

(34) Xu, Z.; Chen, L. M.; Chen, M. H.; Li, G.; Yang, Y. Energy level alignment of poly(3-hexylthiophene):[6,6]-phenyl C_{61} butyric acid methyl ester bulk heterojunction. *Appl. Phys. Lett.* **2009**, 95, 013301-3.

(35) Nayak, P. K.; Periasamy, N. Calculation of electron affinity, ionization potential, transport gap, optical band gap and exciton binding energy of organic solids using 'solvation' model and DFT. *Org. Electron.* **2009**, 10, 1396–1400.

(36) Schwenn, P. E.; Burn, P. L.; Powell, B. J. Calculation of solid state molecular ionization energies and electron affinities for organic semiconductors. *Org. Electron.* **2011**, 12, 394–403.

(37) Rand, B. P.; Genoe, J.; Heremans, P.; Poortmans, J. Solar cells utilizing small molecular weight organic semiconductors. *J. Prog. Photovolt: Res. Appl.* **2007**, 15, 659–676.

(38) Norton, J. E.; Brédas, J. L. Polarization energies in oligoacene semiconductor crystals. *J. Am. Chem. Soc.* **2008**, 130, 12377–12384.

(39) Li, Y.; Pullerits, T.; Zhao, M.; Sun, M. Theoretical characterization of the $PC_{60}BM$: PDDTT model for an organic solar cell. *J. Phys. Chem. C* **2011**, 115, 21865–21873.

(40) Adamo, C.; Barone, V. Exchange functionals with improved long-range behavior and adiabatic connection methods without adjustable parameters: The mPW and mPW1PW models. *J. Chem. Phys.* **1998**, 108, 664–675.

(41) Bérubé, N.; Gosselin, V.; Gaudreau, J.; Côté, M. Designing polymers for photovoltaic applications using ab initio calculations. *J. Phys. Chem. C* **2013**, 117, 7964–7972.

(42) Liu, X.; Shen, W.; He, R.; Luo, Y.; Li, M. Strategy to modulate the electron-rich units in donor-acceptor copolymers for improvements of organic photovoltaics. *J. Phys. Chem. C* **2014**, 118, 17266–17278.

(43) Guo, X.; Zhou, N.; Lou, S.; Smith, J.; Tice, D.; Hennek, J.; Ortiz, R.; Navarrete, J. T. L.; Li, S.; Strzalka, J.; Chen, L.; Chang, R. P. H.; Facchetti, A.; Marks, T. J. Polymer solar cells with enhanced fill factors. *Nat. Photonics.* **2013**, 7, 825–833.

(44) Gupta, D.; Mukhopadhyay, S.; Narayan, K. Fill factor in organic solar cells. *Sol. Energy Mater. Sol. Cells.* **2010**, 94, 1309–1313.

(45) Zhou, Y.; Fuentes-Hernandez, C.; Shim, J. W.; Khan, T. M.; Kippelen, B. High performance polymeric charge recombination layer for organic tandem solar cells. *Energy Environ. Sci.* **2012**, 5, 9827–9832.

(46) Liu, X.; Huang, C.; Shen, W.; He, R.; Li, M. Theoretical investigations on enhancing the performance of terminally diketopyrrolopyrrole-based

small-molecular donors in organic solar cell applications. *J. Mol. Model.* **2016**, 22, 15-11.
(47) Green, M. A. Solar cell fill factors: general graph and empirical expressions. *Solid-State Electron.* **1981**, 24, 788–789.
(48) Kippelen, B.; Brédas, J. L. Organic photovoltaics. *Energy Environ. Sci.* **2009**, 2, 251–261.
(49) Ardo, S.; Meyer, G. J. Photodriven heterogeneous charge transfer with transition-metal compounds anchored to TiO_2 semiconductor surfaces. *Chem. Soc. Rev.* **2009**, 38, 115–164.
(50) Smestad, G. P.; Grätzel, M. Demonstrating electron transfer and nanotechnology: a natural dye-sensitized nanocrystalline energy converter. *J. Chem. Educ.* **1998**, 75, 752–756.
(51) Lemaur, V.; Steel, M.; Beljonne, D.; Brédas, J. L.; Cornil, J. Photoinduced charge generation and recombination dynamics in model donor/acceptor pairs for organic solar cell applications: a full quantum-chemical treatment. *J. Am. Chem. Soc.* **2005**, 127, 6077–6086.
(52) Van Rysselberghe, P. Remarks concerning the Clausius-Mossotti law. *J. Phys. Chem.* **1932**, 36, 1152–1155.
(53) Zang, D. Y.; So, F. F.; Forrest, S. R. Giant anisotropies in the dielectric properties of quasi-epitaxial crystalline organic semiconductor thin films. *Appl. Phys. Lett.* **1991**, 59, 823–825.
(54) Brocks, G.; van den Brink, J.; Morpurgo, A. F. Electronic correlations in oligo-acene and -thiopene organic molecular crystals. *Phys. Rev. Lett.* **2004**, 93, 146405–4.
(55) Mihailetchi, V. D.; van Duren, J. K. J.; Blom, P. W. M.; Hummelen, J. C.; Janssen, R. A. J.; Kroon, J. M.; Rispens, M. T.; Verhees, W. J. H.; Wienk, M. M. Electron transport in a methanofullerene. *Adv. Funct. Mater.* **2003**, 13, 43–46.
(56) Zhang, M. X.; Chai, S.; Zhao, G. J. BODIPY derivatives as n-type organic semiconductors: isomer effect on carrier mobility. *Org. Electron.* **2012**, 13, 215–221.
(57) Marcus, R. A. Theory of electron-transfer reaction rates of solvated electrons. *J. Chem. Phys.* **1965**, 43, 3447–3489.
(58) Lorentz, H. A. Über die beziehungzwischen der fortpflanzungsgeschwindigkeit des lichtes der Körperdichte. *Ann. Phys.* **1880**, 9, 641–665.
(59) Lorenz, L. Über die refractionsconstante. *Ann. Phys.* **1880**, 11, 70–103.
(60) Yin, S.; Yi, Y.; Li, Q.; Yu, G.; Liu, Y.; Shuai, Z. Balanced carrier transports of electrons and holes in silole-based compounds-a theoretical study. *J. Phys. Chem. A* **2006**, 110, 7138–7143.
(61) Troisi, A.; Orlandi, G. Hole migration in DNA: a theoretical analysis of the role of structural fluctuations. *J. Phys. Chem. B* **2002**, 106, 2093–2101.
(62) Yin, S.; Li, L.; Yang, Y.; Reimers, J. R. Challenges for the accurate simulation of anisotropic charge mobilities through organic molecular crystals: The β phase of mer-tris(8-hydroxyquinolinato)aluminum (III) (Alq3) crystal. *J. Phys. Chem. C* **2012**, 116, 14826–14836.
(63) Zhao, C. B.; Ge, H. G.; Zhang, Q.; Jin, L. X.; Wang, W. L.; Yin, S. W. Theoretical investigation on photovoltaic properties of the BBPQ-PC_{61}BM system. *Acta Phys. Chim. Sin.* **2016**, 32, 2503–2510.
(64) Liu, T.; Troisi, A. What makes fullerene acceptors special as electron acceptors in organic solar cells and how to replace them? *Adv. Mater.* **2013**, 25, 1038–1041.
(65) Marcus, R. A. Electron transfer reactions in chemistry. Theory and experiment. *Rev. Mod. Phys.* **1993**, 65, 599–610.
(66) Marcus, R. A. Chemical and electrochemical electron-transfer theory. *Ann. Rev. Phys. Chem.* **1964**, 15, 155–196.
(67) Listorti, A.; O'Regan, B.; Durrant, J. R. Electron transfer dynamics in dye-sensitized solar cells. *Chem. Mater.* **2011**, 23, 3381–3399.
(68) Arbogast, J. W.; Foote, C. S.; Kao, M. Electron transfer to triplet fullerene C_{60}. *J. Am. Chem. Soc.* **1992**, 114, 2277–2279.
(69) Sariciftci, N. S.; Smilowitz, L.; Heeger, A. J.; Wudi, F. Photoinduced electron transfer from a conducting polymer to buckminsterfullerene. *Science.* **1991**, 253, 1474–1476.
(70) Einstein, A. Über die von der molekularkinetischen theorie der wärme geforderte bewegung von in ruhenden flüssigkeiten suspendierten teilchen. *Ann. Phys.* **1905**, 322, 549–560.
(71) van Smoluchowski, M. Zur kinetischen theorie der brownschen molekularbewegung und der suspensionen. *Ann. Phys.* **1906**, 21, 756–780.
(72) Huang, J. D.; Wen, S. H.; Deng, W. Q.; Han, K. L. Simulation of hole mobility in α-oligofuran crystals. *J. Phys. Chem. B* **2011**, 115, 2140–2147.
(73) Peng, Q.; Yi, Y.; Shuai, Z.; Shao, J. Toward quantitative prediction of molecular fluorescence quantum efficiency: role of duschinsky rotation. *J. Am. Chem. Soc.* **2007**, 129, 9333–9339.

Theoretical Prediction of the Photovoltaic Properties of BFBPD-$PC_{61}BM$ System as a Promising Organic Solar Cell

ZHAO Cai-Bin(赵蔡斌)　MA Jian-Qi(马剑琪)　GE Hong-Guang(葛红光)

TANG Zhi-Hua(唐志华)　JIN Ling-Xia(靳玲侠)　WANG Wen-Liang(王文亮)

The photovoltaic properties of BFBPD-$PC_{61}BM$ system as a potential high-performance organic solar cell were theoretically investigated by means of quantum chemistry and molecular dynamics calculations coupled with the incoherent charge-hopping model.